Evaluation of microporous hollow fibre membranes for mass transfer of H_2 into anaerobic digesters for biomethanisation

W.J. Nock[a,*], A. Serna Maza[b], S. Heaven[c], C.J. Banks[c]

[a] *Element Energy, Suite 1, Bishop Bateman Court, Cambridge, CB5 8AQ, United Kingdom*
[b] *URBASER S.A., R & D and Innovation Department, Camino de las Hormigueras 171, 28031, Madrid, Spain*
[c] *Faculty of Engineering and the Environment, University of Southampton, Highfield, Southampton, SO17 1BJ, United Kingdom*

Abstract

BACKGROUND: With high surface-to-volume ratios, hollow fibre membranes offer a potential solution to improve gas-liquid mass transfer. This work experimentally determined the mass transfer characteristics of commercially available microporous hollow fibre membranes and compared this with the mass transfer from bubble column reactors. Both mass transfer systems are considered for biological methanisation, a process that faces a challenge to enhance the H_2 gas-liquid mass transfer for methanogenic Archaea to combine H_2 and CO_2 into CH_4.

RESULTS: Polypropylene membranes showed the highest mass transfer rate of membranes tested, with a mass transfer coefficient for H_2 measured as $k_L = 1.210^{-4}\ m\ s^{-1}$. These results support the two-film gas-liquid mass transfer theory, with higher mass transfer rates measured with an increase in liquid flow velocity across the membrane. Despite the higher mass transfer rate from polypropylene membranes and with a liquid flow across the membrane, a volumetric surface area of $\alpha = 10.34\ m^{-1}$ would be required in a full-scale in-situ

* *Email address:* williamnock88@gmail.com (W.J. Nock)

This article has been accepted for publication and undergone full peer review but has not been through the copyediting, typesetting, pagination and proofreading process, which may lead to differences between this version and the Version of Record. Please cite this article as doi: 10.1002/jctb.6081

biological methanisation process with much larger values potentially required for high-rate ex-situ systems.

CONCLUSIONS: The large surface area of hollow fibre membranes required for H_2 mass transfer and issues of fouling and replacement costs of membranes are challenges for hollow fibre membranes in large-scale biological methanisation reactors. Provided the initial bubble size is small enough ($d_e < 0.5mm$) calculations indicate that microbubbles could offer a simpler means of transferring the required H_2 into the liquid phase at a head typical of that found in commercial-scale anaerobic digesters.

Keywords: biomethanisation, carbon dioxide, hydrogen, methane, mass transfer, power-to-gas

1. Introduction

Gas-liquid mass transfer rates are important in a wide variety of chemical and biological processes and mass transfer design needs to consider a range of factors specific to the application, including the scale and dimensions of the reactor, sensitivity of biological cells to shear forces, reaction rate and process economics. An important development in meeting these requirements is the application of new membrane materials configured as novel types of gas diffuser. These have the potential to increase gas-liquid mass transfer while avoiding the use of energy-intensive mixing systems and high flow rates in the gaseous phase, both of which can affect performance and increase operating costs.

One such process that depends on gas transfer is the biological methanisation of CO_2. This reaction has attracted considerable commercial interest recently, as it offers a possible route to energy storage via the conversion of renewable electricity into H_2 and then to CH_4 [1]. The conversion process utilises hydrogenotrophic methanogenic Archaea [2], and may be conducted in-situ within an anaerobic digester, with H_2 added to combine with CO_2 in the biogas [3, 4];

or ex-situ in a separate hydrogentrophic reactor, using gaseous feedstocks of H_2 and CO_2 [5, 6] or H_2 and biogas [7]. Ex-situ reactors typically have higher volumetric conversion rates from H_2/CO_2 to CH_4 than in-situ reactors [8]. Biological gas upgrading by either of these methods has the potential to reduce both the costs and the methane slippage characteristic of existing physico-chemical biogas upgrading technologies [9], and may also provide a future tool for carbon capture and utilisation.

Due to the low solubility of H_2 and the reaction stoichiometry (4:1; see equation 1), gas-liquid mass transfer is the limiting step for this process and as such is recognised as a major engineering challenge [1]. Research work conducted at laboratory and pilot scale has experimented with a range of different mass transfer approaches for H2 into biological methanisation reactors. Given the mainly pre-commercial stage of this technology the most effective mass transfer process for full-scale systems has yet to be determined, and mass transfer approaches used in laboratory scale experiments may not be the most suited to full-scale operation.

$$4H_2 + CO_2 \rightarrow CH_4 + 2H_2O \tag{1}$$

The range of reactor types that has been tested for biological methanisation includes continuous stirred tank reactors (CSTR) [10], fixed bed reactors [6] and hollow fibre membrane bioreactors [5]. Kougias et al. evaluated the gas conversion efficiency of CSTR, serial upflow reactors and bubble columns for biogas upgrading by addition of externally-produced H_2, CH_4 and CO_2 to a mixed culture of hydrogenotrophic methanogens. Methane concentrations of $> 98\%$ were achieved in the upflow reactor series and bubbling reactor due to the greater gas-liquid contact time and improved gas to liquid mass transfer. To improve mass transfer from bubbles, previous researchers have also used

impellers to increase liquid phase mixing and turbulence [11, 12, 13, 14, 15]. This approach, however, is likely to have considerable implications for the energy consumption on scale-up [1].

Hollow fibre membranes have been investigated for the supply of gases into fermenters, including research from Ju et al. [5], Orgill et al. [16] and Yasin et al. [17]. Hollow fibre membranes have the advantage that mass transfer occurs at the membrane surface, so that gaseous components have already transferred into the liquid phase when exiting the membrane, and thus there are no losses of the gas species. This is in contrast to bubbling, where losses may occur if the gas is not completely absorbed before the bubble reaches the surface.

For hollow fibre membranes to enhance gas-liquid mass transfer during biomethanisation correct selection of membrane material, characteristics and system configuration is essential. In the current work mass transfer coefficients were compared for four different commercial hollow fibre membranes, with the effect of gas species, gas flow rates, gas pressure in the membrane lumen and liquid cross-flow velocities considered for a selected membrane type. Experimental work was conducted using tap water to compare the physical mass transfer effectiveness of different membrane systems, without the added complexities and dynamics of a biological system. Additionally, the reactor system as a whole needs to be considered from the viewpoint of scale-up, which will affect a number of gas transfer parameters. The performance of the most suitable microporous hollow fibre membrane tested was thus compared with simulated results for bubbled systems at an operational scale.

2. Methods

2.1. Mass transfer calculations

The mass transfer rate is a critical design parameter for gas-liquid mass transfer systems, such as hollow fibre membrane contactors. The mass transfer rate is defined as the change in concentration with time and is shown in equation 2 for liquid side controlled mass transfer.

$$\frac{d[C]}{dt} = K_L\alpha([C^*] - [C_0]) \tag{2}$$

Where $[C]$ is the concentration of the dissolved gas, K_L $(m\ s^{-1})$ is the overall liquid side mass transfer coefficient, α (m^{-1}) is the volumetric gas-liquid contact area and $([C^*]-[C_0])$ is the concentration difference across the gas-liquid interface.

As shown by equation 2 the change in concentration with time is a function of the mass transfer coefficient, and integration of equation 2 with respect to time results in the mass transfer coefficient expressed by equation 3, based on the calculation methodology detailed previously by Mendoza et al. [18].

$$K_L\alpha.t = ln\frac{([C^*] - [C_{t=0}])}{([C^*] - [C])} \tag{3}$$

Where t is time, $[C^*]$ is the saturated concentration of the gas species in the liquid, $[C_{t=0}]$ is the initial concentration of the gas species and $[C]$ is the concentration at time t.

The volumetric surface area from equation 2 can be used to find the required membrane area for a given reactor volume (*i.e.* $\alpha \times$ reactor volume) provided the overall liquid side mass transfer coefficient K_L and the concentration driving force $([C^*] - [C_0])$ are known. In this case the dissolved concentration of H_2 in the liquid phase $[C_0]$ can be assumed as 0, as the dissolved H_2 will be consumed

by the methanogenic Archaea. The concentration of H_2 from the gas phase can be determined by the partial pressure of H_2 in the gas phase and Henry's Law, and this will provide the concentration driving force for mass transfer. The overall liquid side mass transfer coefficient can be calculated from experimental data or from empirical correlations such as those from Yang and Cussler [19], Ferreira et al. [20] or Ahmed et al. [21].

Mass transfer theory indicates that a species transferring from the gas phase across a hollow fibre membrane to the liquid phase is required to overcome resistance from the gas side and the liquid side as well as the membrane [22]. This can be quantified by the mass transfer coefficients, where the total mass transfer coefficient is the sum of the mass transfer coefficients shown in equations 4 and 5.

Non-wetted membrane pores:

$$\frac{1}{K_L} = \frac{1}{Hk_G} + \frac{1}{Hk_M} + \frac{1}{k_L} \tag{4}$$

Wetted membrane pores:

$$\frac{1}{K_L} = \frac{1}{Hk_G} + \frac{1}{k_M} + \frac{1}{k_L} \tag{5}$$

In this case k_G, k_L and k_M are the gas, liquid and membrane coefficients, respectively, while H ($mol\ L^{-1}\ atm^{-1}$) is Henry's law coefficient of the gas species in the liquid phase, listed in Table 1 for the gases tested in this work. The solubility of H_2 in water is very low, thus H_2 has a large Henry's law coefficient, and this results in the resistance to mass transfer being significantly larger on the liquid side than the gas side. The magnitude of the membrane resistance k_M is dependent on the degree of wettedness of the membrane pores [23].

Table 1: Henry's Law coefficient for O_2, CO_2 and H_2, taken for water at 298 K, from Sander [24]

Gas	**Henry's Law coefficient**
O_2	$4.36 \times 10^6\ kPa$
CO_2	$0.16 \times 10^6\ kPa$
H_2	$7.19 \times 10^6\ kPa$

Table 2: Hollow fibre membrane properties

Manufacturer	**Material**	**Outer diameter**	**Pore size**
Suzhou Flylong Technology	polyvinylidene fluoride ($PVDF$)	300 μm	0.1 μm
Yuasa Membrane Systems	polysulfone (PS)	800 μm	0.04 μm
Zena Membranes	polypropylene (PP # 1)	300 μm	0.1×0.5 μm
Membrana (3M)	polypropylene (PP # 2)	380 μm	0.2 μm

2.2. Membranes and experimental set-up

The properties of the four different commercial hollow fibre membranes for which the mass transfer performance was characterised are shown in Table 2. The mass transfer rate was determined for three gases; O_2, H_2 and CO_2 absorbing in tap water with the experimental set-up shown in figure 1.

The overall mass transfer coefficient (shown in equations 4 and 5) can be compared with different gases based on Henry's coefficient. The testing of three gases allows for a comparison of the overall mass transfer effectiveness of the system. In this case dissolved oxygen was measured in-line with a dissolved oxygen probe, while dissolved CO_2 and dissolved H_2 were measured off-line from a sample, with the gas and liquid concentrations allowed to equilibrate before measurement of the gas concentration and calculation of the liquid concentration from Henry's Law.

Gas concentrations and the input and output gas volumes were measured to provide a gas phase mass balance to be combined with the measurements of the

dissolved gases to provide an overall mass balance of the experiments. The gas volume was measured using a weight-type gasometer according to Walker et al. and reported at a standard temperature and pressure (STP) of 0 ^oC and 101.3 kPa.

Gas concentrations were analysed using a gas chromatograph (Varian CP-3800, Varian Medical Systems, US) with a gas sampling loop using argon (BOC, UK) as the carrier gas at a flow rate of 50 $ml\ min^{-1}$. The gas chromatograph was fitted with a Hayesep C column and a molecular sieve $13 \times (80 - 100$ mesh) operating at a temperature of 50^oC.

The hollow fibre membranes were potted with epoxy resin into a linear configuration inside two acrylic fixings with gas inlets/outlets connected at each end. Figure 1c shows an image of the 3 mm hollow fibre membranes. Before each experiment gas-impermeable sampling bags were filled with the desired gas (O_2, H_2, and CO_2; BOC, UK), which was then pumped into the hollow fibre membrane fixing with a peristaltic pump (Watson Marlow, UK). When operating at atmospheric pressure the output gas was collected in an outlet gas sampling bag. For experiments with a pressurised gas phase the inlet gas line was divided in two, with both inlet lines connected to the hollow fibre fixings. A pressure transducer (Hydrotechnik, UK) was connected to the inlet gas line to measure the gas pressure. The hollow fibre fixing was located in the centre of the reactor, and could be positioned in different configurations. Tap water was used as the liquid phase, which was recirculated with a centrifugal pump (CEB103, Clarke, UK).

For the experiments with O_2, the dissolved oxygen (DO) concentration was measured with a dissolved oxygen meter (ENV-40-DO, Atlas Scientific, US). During CO_2 experiments the pH was measured using a glass bulb pH electrode (Extech, UK) calibrated with buffer solutions at pH 4 and pH 7. DO and

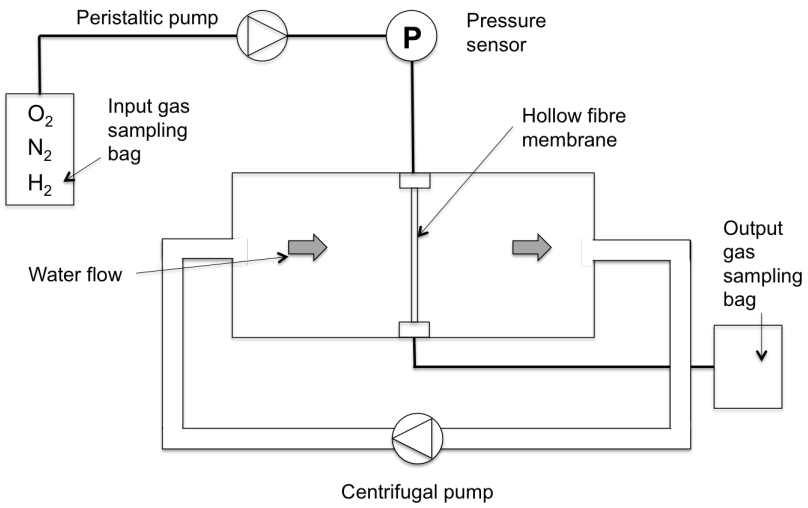

(a) Schematic of the experimental set-up

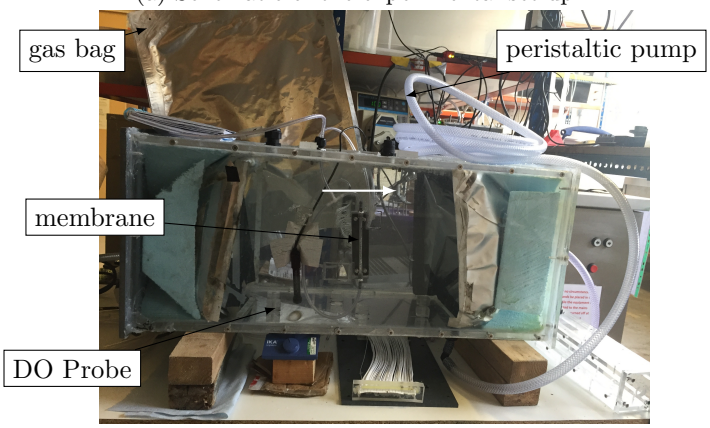

(b) Photograph of the experimental set-up

(c) Image of the membrane fixing and potting used to secure the hollow fibre membranes

Figure 1: Experimental set-up to measure mass transfer rate from hollow fibre membranes

pH data were acquired continuously using a LabJack U6 (LabJack, US) and a Raspberry Pi (Raspberry Pi Foundation, UK) was used to log the data.

Liquid samples for dissolved H_2 and CO_2 were taken over time intervals to determine the rate of change in dissolved gas concentrations, as shown by equation 2. Serum bottles (50 mL) were half filled with liquid and sealed with a crimp top. After weighing, the samples were placed on an orbital shaker at 20^oC for two hours to ensure the gas concentration in the headspace had equilibrated. A 10 mL gas sample was then extracted with a syringe and analysed using a gas chromatograph as detailed above.

3. Results & Discussion

Figure 2 shows the overall liquid side mass transfer coefficients (K_L) measured for the four microporous hollow fibre membrane materials tested with O_2 under atmospheric pressure absorbing into still tap water. The polyvinylidene fluoride (PVDF) and polysulfone (PS) membranes showed lower K_L than the polypropylene (PP) membranes. This is due to the hydrophilic properties of the PVDF and PS membranes. Commercially available PP membranes are highly hydrophobic, while PS and PVDF membranes have lower hydrophobicity [26]. Contact angles for these membranes have been reported in the literature, with average values reported for PP, PVDF and PS of 102.1°, 89° and 70.5°, respectively [27]. The lower contact angle of the PS and PVDF polymers allows more water to fill the membrane pores, resulting in the lower overall liquid side mass transfer coefficients of these membranes (as a result of k_M in equation 5).

The PS membranes have a smaller pore size than the PVDF membranes and, along with different hydrophilicities, this could play a role in reducing the wettedness of the PS pores. Both of the PP membranes showed higher mass transfer coefficients (K_L) for O_2 mass transfer. PP #1 corresponding to the

hollow fibre membrane from Zena Membranes showed a slightly lower mass transfer coefficient (K_L) than PP #2 from Membrana. These PP membranes are hydrophobic, which will reduce the water content and 'wettedness' of the membrane pores. The membranes from Membrana (PP #2) have a smaller pore size than those from Zena Membranes (PP #1): this could result in a lower 'wettedness' and thus explain the higher mass transfer coefficient (K_L).

It should also be noted from figure 2 that increasing the gas flow rate from 0.2×10^{-6} to 1.2×10^{-6} m^3 s^{-1} did not have any noticeable effect on the mass transfer coefficient. This provides support for the theory that the mass transfer of O_2, a low solubility gas, is dominated by the liquid side mass transfer coefficient (k_L), with a negligible contribution from the gas side mass transfer coefficient (k_G).

When the pressure difference between the gas phase and the liquid phase either side of the membrane is greater than the membrane wetting pressure, the membrane pores can be assumed to be non-wetted. The overall liquid side mass transfer coefficient (K_L) can then be calculated assuming negligible mass transfer resistance from the membrane, as shown in equation 4. Figure 3 shows the effect of increasing the gas pressure of O_2 on K_L for the polypropylene Membrana membrane (PP # 2). This is shown with still liquid ($u_L = 0\ ms^{-1}$), and with a liquid flow across the membrane ($u_L = 1.2 \times 10^{-3}\ ms^{-1}$). There is an increase in K_L with an increase in pressure for a still liquid and with a liquid flow velocity, up to a pressure between $1.5 - 2$ bar (absolute pressure). Above this pressure, the overall liquid side mass transfer coefficient appears to remain relatively constant. This is shown more clearly where there is a liquid velocity across the membrane, and a greater increase in overall liquid side mass transfer coefficient with pressure. The higher gas pressure will maintain an un-wetted pore. The pressure at which the pores remain un-wetted will be dependent on

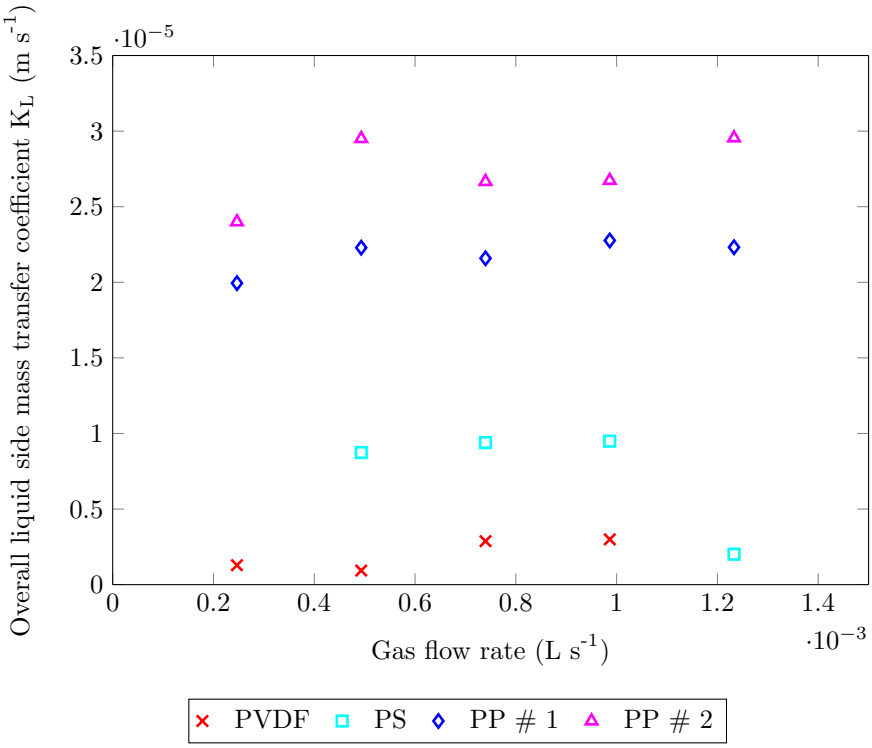

Figure 2: Overall liquid side mass transfer coefficient for O_2 under atmospheric pressure into still tap water for different commercial membranes

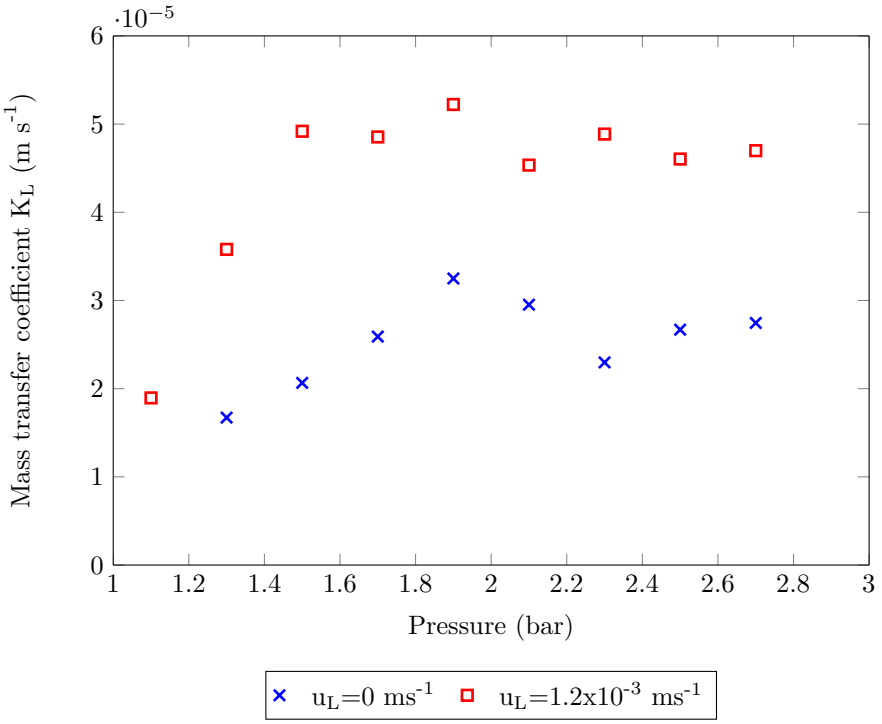

Figure 3: Mass transfer coefficient for O_2 under pressure into tap water through Membrana PP membranes (PP # 2) under still and flowing liquid

the hollow fibre membrane material properties (hydrophobicity) and the pore size: for the polypropylene Membrana membrane (PP # 2) this is between $1.5 - 2$ bar (absolute pressure).

Figure 4 shows the effect of increasing the liquid flow velocity on the mass transfer coefficient, with the hollow fibre membranes positioned perpendicular to the direction of the flow. There is a clear increase in the overall liquid side mass transfer coefficient for O_2 with liquid velocity across the hollow fibre membrane. This corresponds with results from previous studies, such as Yang and Cussler [19], Ahmed et al. [21] and Zhang et al. [28]. Considering the two-film theory for gas-liquid mass transfer, a higher liquid velocity results in a shallower liquid film and lower overall liquid side mass transfer coefficient. This suggests that for these hydrophobic membranes and at the liquid velocities considered in this

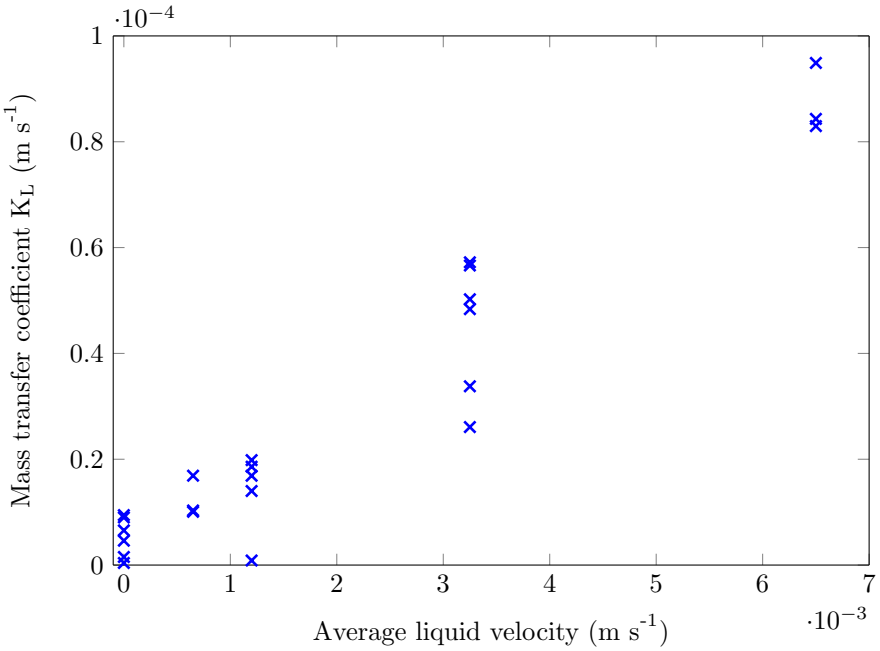

Figure 4: Mass transfer coefficient for O_2 at atmospheric pressure into tap water through PP membranes at different liquid cross-flow velocities

work the mass transfer of O_2 into water is controlled from the liquid side, with the liquid properties strongly affecting the mass transfer. Yang and Cussler noted that using a hydrophilic membrane, in which the pores will be filled with water, leads to a higher membrane resistance, and therefore the liquid side mass transfer resistance is of less importance for the overall mass transfer rate [19].

These experiments were repeated for the mass transfer of CO_2 and H_2 across the polypropylene hollow fibre membrane (PP # 2). Table 3 shows the mass transfer coefficients recorded with a liquid flow velocity of $u_L = 6.5 \times 10^{-3}\ m\ s^{-1}$ across the membrane. The overall liquid side mass transfer coefficient for H_2 is slightly higher than that of O_2, due to the higher liquid diffusivity of H_2 [29].

Table 3: Overall liquid side mass transfer coefficient for O_2, CO_2 and H_2 through polypropylene hollow fibre membrane (PP # 2)

Gas	**Overall liquid side mass transfer coefficient** (K_L)	**Liquid flow velocity**	**Pressure**
O_2	9.49×10^{-5} m s^{-1}	6.5×10^{-3} m s^{-1}	1.0 bar
CO_2	1.08×10^{-5} m s^{-1}	6.5×10^{-3} m s^{-1}	1.0 bar
H_2	1.24×10^{-4} m s^{-1}	6.5×10^{-3} m s^{-1}	1.0 bar

3.1. Scale-up for biomethanisation

The mass transfer coefficients from the experimental results section can be used to find the area of microporous hollow fibre membrane required to supply H_2 for biomethanisation. Table 4 shows the design requirement for a 500 m^3 anaerobic digester. The H_2 requirement has been assumed from a biogas production rate of 1 L biogas $\mathrm{L}^{-1}\mathrm{day}^{-1}$ with a CO_2 content of 50 %. Taking the stoichiometric ratio of four moles of H_2 per mole of CO_2 as shown in equation 1 the total H_2 requirement is 1 000 m^3 day^{-1}.

The volumetric membrane area (i.e. membrane area in m^2 per unit volume m^3) required to provide the 1 000 m^3 day^{-1} into the 500 m^3 reactor can be calculated from equation 2. The required mass transfer rate is 1 000 m^3 day^{-1}. When converted to moles using the Ideal gas law and expressed per litre of reactor this is 9.63×10^{-7} $mols$ $(L.s)^{-1}$. The concentration difference and driving force for the mass transfer is taken from Henry's Law for H_2 at 7.8×10^{-4} mol L^{-1}. The mass transfer coefficient is based on favourable mass transfer conditions and taken as $K_L = 1.2 \times 10^{-4}$ m s^{-1} for the Membrana membranes (PP # 2). Inserting these values into equation 2 results in a required volumetric membrane area (α) of 10.34 m^{-1}. Scaling this up based on the reactor volume would result in a total membrane area of 5 170 m^2 for a 500 m^3 reactor. Considering the membrane diameter is 380 μm this equates to a membrane length of 8 660 m m^{-3}.

The overall liquid side mass transfer coefficient taken in this example de-

Table 4: Hollow fibre membrane design requirement for H_2 mass transfer into an anaerobic digester for biomethanation

Parameter	**Value**
Reactor volume	500 m^3
Reactor height	8 m
H_2 flow rate	700 $L\ min^{-1}$
Mass transfer coefficient (K_L)	$1.2 \times 10^{-4}\ m\ s^{-1}$
Volumetric surface area	10.34 m^{-1}
Total surface area	5170 m^2

sign calculation was measured with a liquid flow across the membrane of $6.5 \times 10^{-3}\ m\ s^{-1}$, with the H_2 gas phase pumped through the membrane at atmospheric pressure. Higher mass transfer coefficients could be achieved at greater pressures and liquid flow velocities across the hollow fibre membrane; however this would come with higher energy requirements and therefore higher operating costs.

Grasso et al. [13] and Strevett et al. [14] studied mass transfer through hollow fibre membrane modules located outside the main reactor, with liquid pumped through the module. For a 2 L working volume reactor they employed a membrane surface area 0.622 m^2 or 3208 $m^2\ m^{-3}$ (2500 $fibres \times 0.33\ m \times 240\ \mu m\ \oslash$). Grasso et al. [13] compared the mass transfer characteristics of this system with that of a porous metal diffuser and found the larger volumetric gas-liquid area of the hollow fibre membranes improved mass transfer performance. Luo and Angelidaki [4] placed a hollow fibre membrane module inside a CSTR: for a working volume of 0.6 L they employed a surface area of 0.071 m^2 (400 $fibres \times 0.2\ m \times 284\ \mu m\ \oslash$). In this case biofilm forming on the membrane surface was found to have an adverse effect on the process by increasing the resistance to diffusion of H_2 into the liquid. One disadvantage of hollow fibre membranes in comparison to bubbled systems is their relatively limited operating lifespan, particularly in systems prone to fouling such as anaerobic digesters: periodic cleaning and replacement is likely to be required, resulting in higher operation

and maintenance costs [30].

3.2. Comparison with bubbled systems

An important advantage of using hollow fibre membranes for gas-liquid mass transfer is the complete transfer of the gas species on crossing the membrane. This is in contrast to bubbled systems, which have a gas-liquid contact time dependent on the reactor height and bubble rise velocity and, as a result, risk incomplete mass transfer of the gas species to the liquid phase when the bubble reaches the liquid surface. In such a scenario the headspace could be recirculated and bubbled back through the digester liquor to allow further H_2 mass transfer. The presence of CH_4 and CO_2 in the headspace would greatly diminish the concentration driving force for H_2 mass transfer, however, although there could be benefits in providing further mixing of the reactor through additional bubbling.

To estimate the extent of H_2 losses from bubbled systems, simulations were carried out to calculate the mass transfer of H_2 into water for different bubble sizes. These simulations are only approximate, and the counter-diffusion of dissolved gases (such as CO_2 and CH_4) was assumed to be negligible. The experiments in this work used tap water; similarly the simulations were based on the properties of tap water. A comparison between the physical properties of tap water and digester liquor is given in table 5. There is only a small density difference between digester liquor and water, which is affected by the solids content of the feedstock, and is unlikely to have a significant effect on mass transfer. The liquid density does affect the viscosity, which is noticeably different between tap water and digester liquor. The higher dynamic viscosity of digester liquor would reduce the mass transfer rate due to a lower gas-liquid diffusivity. This was shown by Fernández et al. [31] who replicated the rheological characteristics of digestate in a 2.0 m bubbling tower with glycerol and carboxymethyl cellulose

Table 5: Comparison between properties of tap water and digester liquor values reported from the literature or where stated from experimental measurement

Parameter	**Tap water**	**Digester liquor**	**Source**
Density* ($kg\ m^{-3}$)	998	$997 - 1023$**	Experimental measurement
Viscosity* ($kg\ m^{-1}s^{-1}$)	$1\ \times\ 10^{-3}$	$2.1-3.3\ \times\ 10^{-3}$	Tixier et al. [33]
Surface tension* ($N\ m^{-1}$)	$73\ \times\ 10^{-3}$	$33-46\ \times\ 10^{-3}$	Elmitwalli et al. [34]
Temperature (^oC)	$20-25\ ^oC$	$35\ ^oC$ mesophilic or 55^oC for thermophilic	Experimental measurement

* Assumed at 20^oC unless otherwise stated ** Density dependent on solids content within digester

sodium salt, and concluded that an increase in viscosity from 130 to 340 cPo, within the values found in digestate, reduced k_La by 43 %.

The experiments in this work were carried out at room temperature, between $20-25^oC$, which is lower than either the mesophilic (35^oC) or thermophilic (55^oC) temperatures at which anaerobic digesters normally operate. There is a slight reduction in H_2 solubility at higher temperatures, which will therefore reduce the concentration driving force for mass transfer. The presence of surfactant substances is known to have an effect on mass transfer rates from bubbles [32] and these are likely to be present at much higher concentrations in digestates or in the pure cultures of ex-situ biogas upgrading reactors, than in tap water; but the scale of this effect is unknown. Using tap water in the experimental work also prevented fouling of the membrane, ensuring consistent membrane conditions throughout the experiments. In the absence of more data, tap water was therefore considered an acceptable liquid medium for testing purposes.

The mass transfer coefficients used have been calculated based on the theories of mass transfer for a 'mobile' gas-liquid interface taken from Higbie [35] and Montes et al. [36] and an 'immobile' gas-liquid interface from Frössling [37].

Based on previous experimental work by Nock et al. [32] the size of the bubble was used as an indication of whether the gas-liquid interface could be treated as mobile or immobile. The corresponding mass transfer coefficient was then incorporated into a finite difference model. This model calculated the bubble size and rise velocity, taken from Tomiyama et al. [38]. The bubble height and subsequent hydrostatic pressure were then used with the ideal gas law to calculate the mass balance of the bubble with time, as shown in equation 6 where v_B is the bubble volume (m^3), R is the ideal gas constant ($Pa\ m^3\ K^{-1}\ mol^{-1}$), T is temperature (K), y_i is the molar fraction of component i in the gas phase, p_{atm} is atmospheric pressure (Pa), ρ_L the liquid density ($kg\ m^{-3}$), g gravitational acceleration ($m\ s^{-2}$) and z liquid height (m). Based on the mass transfer from single bubbles, this approach allows estimation of the total mass transfer and H_2 losses from the gas phase from bubbles reaching the liquid surface.

$$\frac{dv_B}{dt} = RT \sum \left(\frac{1}{y_i(p_{atm} + \rho_L g z)} \right) K_L \alpha \left(C^* - C_0 \right) \tag{6}$$

From this model, the reduction in H_2 concentration at different bubble diameters is shown in figure 5, which illustrates the significant effect this parameter has on the total mass transfer. With an initial bubble diameter of 3.0 mm, a rise height of approximately 7.0 m would be required for mass transfer of 50 % of the H_2 into the water. Because of its larger volumetric surface area there is a slight improvement in total mass transfer for a smaller initial bubble diameter of 1.0 mm. This difference is small when compared to the mass transfer from microbubbles (defined as $d_B < 1.0\ mm$). A further reduction in initial bubble diameter from 1.0 mm to 0.8 mm has a significant effect. For a bubble with initial diameter of 1.0 mm only 50 % of the H_2 is absorbed after 5.0 m rise height, whereas 80 % is absorbed from the 0.8 mm diameter bubble.

Almost all of the H_2 is absorbed after a 2.0 m rise height with a microbubble

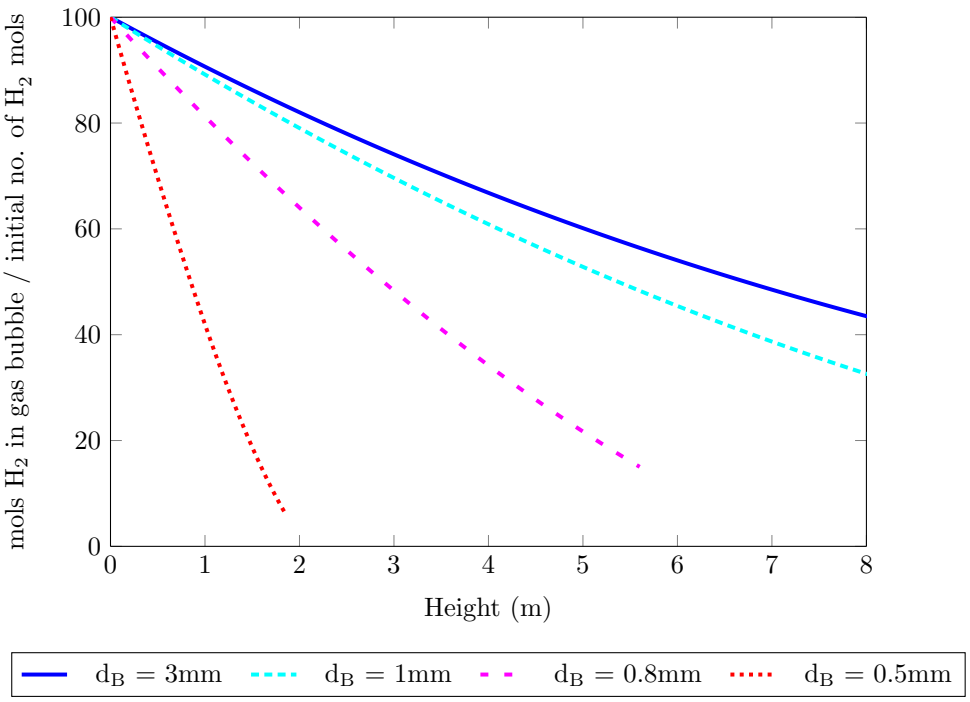

Figure 5: Mass transfer from H_2 bubbles rising through water

of initial diameter 0.5 mm. As the liquid depth in commercial anaerobic reactors is normally greater than 2.0 m, complete H_2 mass transfer from microbubbles could occur under these conditions.

This difference in total mass transfer is due to the bubble rise velocity, which is significantly reduced for microbubbles, as can be seen in figure 6. The reduced bubble rise velocity for bubbles with diameter $d_B < 1.0$ mm results in a longer gas-liquid residence time, which allows the greater overall mass transfer shown in figure 5.

Different options are available with respect to microbubble diffusers. Often an elevated pressure (3.5 bar) is required to produce the microbubbles; in recent research, however, microbubbles have been produced at a reduced input gas pressure and therefore lower energy requirement [39]. The production of

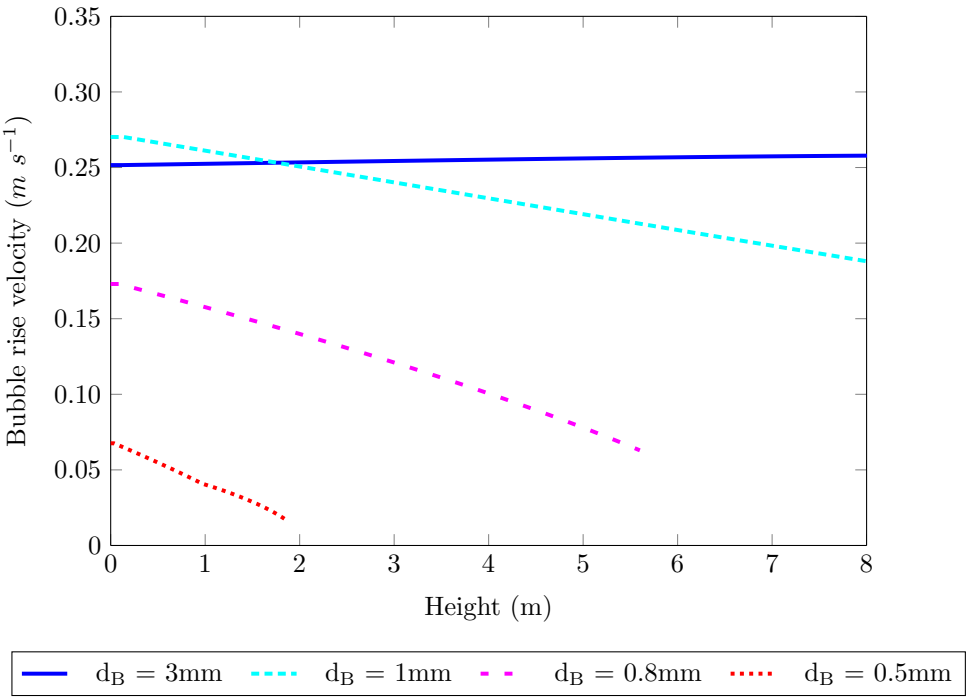

Figure 6: Bubble rise velocity from H_2 bubbles rising through water

microbubbles may also reduce fouling on the gas-liquid membrane, which may be an issue with bubble-less mass transfer from hollow fibre membranes [40].

3.3. Comparison with different membrane systems

As shown in section 3.1, a specific membrane area of 10.3 $m^2\ m^{-3}$ is required to supply H_2 for the in-situ conversion of endogenously-produced CO_2 in a conventional anaerobic digester with a volumetric biogas production rate of 1 $m^3\ m^{-3}\ day^{-1}$ at 50% CO_2 content. The performance of current membranes therefore appears to be adequate at volumetric biogas production rates typical of conventional digesters treating organic wastes or municipal wastewater biosolids. Table 6 gives examples of the use of membranes in anaerobic membrane bioreactors (AnMBRs) for the treatment of liquid effluents, and in biomethanisation studies. Based on these, provision of the specific membrane area for H_2 mass transfer found in this study is feasible. Martin-Garcia et al. [41] utilised a specific membrane area of 10.4 $m^2\ m^{-3}$ in a side-stream membrane unit with a total working volume of 1.2 m^3. Robles et al. [42] used a membrane area of 14.3 $m^2\ m^{-3}$ in a side-stream pilot plant with a total liquid volume of 2.1 m^3. Shin et al. [43] employed 18.2 $m^2\ m^{-3}$ in a 2.7 m^3 submerged AnMBR. On the other hand previous studies with hollow fibre membranes used as diffusers for biological utilisation of H_2 report higher specific membrane areas. Díaz et al. [40] employed 30 $m^2\ m^{-3}$ of membrane in a submerged reactor. Other studies utilised considerably higher specific membrane areas, from 62 to 3208 $m^2\ m^{-3}$ [13, 5, 44, 45, 46]. The higher values for specific membrane surface areas reported in Table 6 reflect the laboratory scale of these studies, and these higher membrane areas maybe less suited to scaling up to pilot and full scale reactors.

Although the membrane area determined from this work is feasible for in-situ CO_2 conversion, current and forthcoming developments in the field of

biomethanisation mean that other types of system may require much higher volumetric gas transfer rates. B et al. [47] demonstrated it was feasible to convert the biogas from three conventional digesters within a single unit in a combined in-situ and ex-situ system. In high-rate ex-situ systems, volumetric methane production rates of 40 m^3 m^{-3} reactor day^{-1} have been achieved at laboratory scale [48], requiring gas inputs of at least 160 and 40 m^3 m^{-3} day^{-1} of H_2 and CO_2, respectively. Methane evolution rates of over 500 L L^{-1} day^{-1} have been demonstrated in short-term operation in chemostat cultivation of pure cultures [2]. If biomethanisation of CO_2 is to make a significant contribution to carbon capture, volumetric methane productivities of this order will be needed in order to minimise reactor size, with correspondingly high rates of mass transfer. A municipal incinerator with a single grate, for example, may produce around 100 000 m^3 CO_2 day^{-1}, while a large cement kiln can produce up to 2.5 million m^3 CO_2 day^{-1}. A biomethanisation reactor with a volumetric conversion rate of 500 m^3 m^{-3} day^{-1} may be a feasible option for the future, but the associated mass transfer rates may require significant advances in membrane performance.

In either case, the use of microbubbles may be preferable when the head of liquid is sufficient to allow optimal H_2 transfer to the liquid, in order to avoid operational problems caused by an increase in pressure resistance due to membrane fouling. Luo et al. [45] reported that the biofilm accumulation on the membrane surface restricted H_2 diffusion and thus consumption. Consequently, the use of membranes for gas transfer may be more suitable in reactors with low liquid head depth, such as pilot plants or laboratory-scale reactors. This could help smaller units maintain a mass transfer performance similar to industrial plants, or as an alternative the H_2-diluted headspace gas could be recirculated through the reactor, providing increased mixing as well as gas-liquid mass transfer.

Table 6: Comparison between anaerobic membrane bioreactors for treatment of liquid effluents and biomethanisation reactors with membranes as bubble-less gas transfer facilitator

Reference	**Vol** (m^3)	**System configuration**	**Membrane material**	**Pore size** (μm)	**OD** (mm)	**Area** (m^2)	**SMA** ($m^2\ m^{-3}$)	**SML** ($m\ m^{-3}$)
AnMBR								
Martin-Garcia et al. [41]	1.2	side-stream	PVDF	0.08	1.3	12.5	10.4	2 551
Martin-Garcia et al. [41]	0.123	side-stream	-	0.04	1.9	0.9	7.6	1 267
Robles et al. [42]	2.1	2 units as side-stream	PES	0.05	2.6	30.0	14.3	1 749
Lew et al. [49]	0.18	side-stream	-	0.2	-	4.0	22.2	-
Gouveia et al. [50]	0.15	submerged post UASB	PVDF	0.045	2.0	0.9	6.2	987
Ramos et al. [51]	0.18	submerged post UASB	PVDF	0.04	2.4	3.5	19.4	2 579
Shin et al. [43]	2.17	submerged post AFBR	PVDF	0.03	-	39.5	18.2	-
Biomethanisation								
Grasso et al. [13]	0.002	side-stream	PP	0.05	0.2	4.7	3 208	412 500
Luo and Angelidaki [4]	0.0006	submerged	PU	-	0.3	0.1	118.8	133 333
Díaz et al. [40]	0.031	submerged	PVDF	0.4	2.3	0.9	30	4 116
Wang et al. [46]	0.002	submerged	PU	-	0.3	0.1	62.4	70 000
Luo and Angelidaki [44]	0.0004	submerged	PP	0.04	0.3	0.1	282.5	300 000

Vol: Volume of reactor OD: Outer membrane diameter Area: Membrane area SMA: Specific membrane area SML: Specific membrane length

4. Conclusion

Biomethanisation utilising hydrogenotrophic methanogens to convert electrolytically produced H_2 with CO_2 from biogas to form CH_4 is a promising approach for energy storage. One current engineering challenge is to enhance the H_2 gas-liquid mass transfer for the methanogens to produce CH_4. This work has characterised the gas-liquid mass transfer from microporous hollow fibre membranes and analysed the potential for scale-up within an anaerobic digester. The large surface area of hollow fibre membranes required may make this approach less attractive, particularly considering issues of fouling and replacement costs of the membranes. Alternatively microbubbles could provide the necessary H_2 into the liquid phase given a sufficient liquid head typical of that found in commercial-scale anaerobic digesters.

5. Acknowledgements

The authors acknowledge the Proof of Concept research grant POC2014011 provided by the Anaerobic Digestion Network (ADNet BB/L013835/1) funded by the Biological and Biosciences Sciences Research Council (BBSRC) and the IB Catalyst project (EP/M028208) funded by the Engineering and Physical Sciences Research Council (EPSRC).

[1] M. Götz, J. Lefebvre, F. Mörs, A. McDaniel Koch, F. Graf, S. Bajohr, R. Reimert, T. Kolb, Renewable Power-to-Gas: A technological and economic review, Renew. Energy 85 (2016) 1371–1390.

[2] S. Rittmann, A. Seifert, C. Herwig, Essential prerequisites for successful bioprocess development of biological CH_4 production from CO_2 and H_2, Crit. Rev. Biotechnol. 35 (2) (2015) 141–151.

[3] G. Luo, S. Johansson, K. Boe, L. Xie, Q. Zhou, I. Angelidaki, Simultaneous hydrogen utilization and in situ biogas upgrading in an anaerobic reactor, Biotechnol. Bioeng. 109 (4) (2012) 1088–1094.

[4] G. Luo, I. Angelidaki, Hollow fiber membrane based H2 diffusion for efficient in situ biogas upgrading in an anaerobic reactor., Appl. Microbiol. Biotechnol. 97 (8) (2013) 3739–44.

[5] D. H. Ju, J. H. Shin, H. K. Lee, S. H. Kong, J. I. Kim, B. I. Sang, Effects of pH conditions on the biological conversion of carbon dioxide to methane in a hollow-fiber membrane biofilm reactor (Hf-MBfR), Desalination 234 (1-3) (2008) 409–415.

[6] J. C. Lee, J. H. Kim, W. S. Chang, D. Pak, Biological conversion of CO 2 to CH 4 using hydrogenotrophic methanogen in a fixed bed reactor, J. Chem. Technol. Biotechnol. 87 (6) (2012) 844–847.

[7] P. G. Kougias, L. Treu, D. P. Benavente, K. Boe, S. Campanaro, I. Angelidaki, Ex-situ biogas upgrading and enhancement in different reactor systems, Bioresource technology 225 (2017) 429—437.

[8] B. Lecker, L. Illi, A. Lemmer, H. Oechsner, Biological hydrogen methanation - A review, Bioresour Technol. 245 (Part A) (2017) 1220–1228.

[9] R. Muñoz, L. Meier, I. Diaz, D. Jeison, A review on the state-of-the-art of physical/chemical and biological technologies for biogas upgrading, Reviews in Environmental Science and BioTechnology 14 (4) (2015) 727–759.

[10] S. Kim, K. Choi, J. Chung, Reduction in carbon dioxide and production of methane by biological reaction in the electronics industry, Int. J. Hydrogen Energy 38 (8) (2013) 3488–3496.

[11] J. P. Peillex, M. L. Fardeau, R. Boussand, J. M. Navarro, J. P. Belaich, Growth of Methanococcus thermolithotrophicus in batch and continuous culture on H2 and CO2: influence of agitation, Appl. Microbiol. Biotechnol. 29 (6) (1988) 560–564.

[12] J. P. Peillex, M. L. Fardeau, J. P. Belaich, Growth of Methanobacterium thermoautotrophicum on H2-CO2: High CH4 productivities in continuous cutlure, Biomass 21 (1990) 315–321.

[13] D. Grasso, K. Strevett, R. Fisher, Uncoupling mass transfer limitations of gaseous substrates in microbial systems, Chem. Eng. J. Biochem. Eng. J. 59 (1995) 195–204.

[14] K. A. Strevett, R. F. Vieth, D. Grasso, Chemo-autotrophic biogas purification for methane enrichment: Mechanism and kinetics, Chem. Eng. J. Biochem. Eng. J. 58 (1) (1995) 71–79.

[15] A. J. Ungerman, T. J. Heindel, Carbon Monoxide Mass Transfer for Syngas Fermentation in a Stirred Tank Reactor with Dual Impeller Configurations, Biotechnology Progress 23 (3) (2007) 613–620.

[16] J. J. Orgill, H. K. Atiyeh, M. Devarapalli, J. R. Phillips, R. S. Lewis, R. L. Huhnke, A comparison of mass transfer coefficients between trickle-bed, hollow fiber membrane and stirred tank reactors, Bioresource Technology 133 (2013) 340 – 346.

[17] M. Yasin, Y. Jeong, S. Park, J. Jeong, E. Y. Lee, R. W. Lovitt, B. H. Kim, J. Lee, I. S. Chang, Microbial synthesis gas utilization and ways to resolve kinetic and mass-transfer limitations, Bioresource Technology 177 (2015) 361 – 374.

[18] J. Mendoza, M. Granados, I. d. Godos, F. Acien, E. Molina, S. Heaven,

C. Banks, Oxygen transfer and evolution in microalgal culture in open raceways, Bioresour Technol. 137 (2013) 188–195.

[19] M. Yang, E. Cussler, Designing Hollow-Fiber Contactors, AIChE J. 32 (11) (1986) 1910–1916.

[20] B. Ferreira, H. Fernandes, A. Reis, M. Mateus, Microporous Hollow Fibres for Carbon Dioxide Absorption: Mass Transfer Model Fitting and the Supply ing of Carbon Dioxide to Microalgal Cultures, J. Chem. Technol. Biotechnol. 71 (1998) 61–70.

[21] T. Ahmed, M. J. Semmens, M. a. Voss, Oxygen transfer characteristics of hollow-fiber, composite membranes, Adv. Environ. Res. 8 (3-4) (2004) 637–646.

[22] Z. Qi, E. Cussler, Microporous hollow fibers for gas absorption ii. Mass transfer across the membrane, J. Memb. Sci. 23 (1985) 333–345.

[23] M. Yasin, S. Park, Y. Jeong, E. Y. Lee, J. Lee, I. S. Chang, Effect of internal pressure and gas/liquid interface area on the CO mass transfer coefficient using hollow fibre membranes as a high mass transfer gas diffusing system for microbial syngas fermentation, Bioresource Technology 169 (2014) 637 – 643.

[24] R. Sander, Compilation of Henry's law constants (version 4.0) for water as solvent, Atmospheric Chemistry and Physics 15 (8) (2015) 4399–4981.

[25] M. Walker, Y. Zhang, S. Heaven, C. Banks, Potential errors in the quantitative evaluation of biogas production in anaerobic digestion processes, Bioresour. Technol. 100 (24) (2009) 6339–6346.

[26] G. Pearce, Introduction to membranes: Membrane selection, Filtration & Separation 44 (3) (2007) 35 – 37.

[27] Accu Dyne Test, https://www.accudynetest.com/polytable_03.html?sortby=contact_angle#branding, accessed: 28 April 2019, 2019.

[28] Z. Zhang, Y. Yan, L. Zhang, S. Ju, Hollow fibre membrane contactor absorption of CO_2 from the flue gas: review and perspective, Global NEST Journal 16 (2) (2014) 354–373.

[29] E. Cussler, Diffusion: Mass transfer in fluid systems, Cambridge University Press, 3rd edition edn., 2009.

[30] A. Gabelman, S.-T. Hwang, Hollow fiber membrane contactors, J. Memb. Sci. 159 (1-2) (1999) 61–106.

[31] Y. B. Fernández, E. Cartmell, A. Soares, E. McAdam, P. Vale, C. Darche-Dugaret, B. Jefferson, Gas to liquid mass transfer in rheologically complex fluids, Chemical Engineering Journal 273 (2015) 656 – 667.

[32] W. Nock, S. Heaven, C. Banks, Mass transfer and gas–liquid interface properties of single CO2 bubbles rising in tap water, Chem. Eng. Sci. 140 (2016) 171–178.

[33] N. Tixier, G. Guibaud, M. Baudu, Determination of some rheological parameters for the characterization of activated sludge, Bioresource Technology 90 (2) (2003) 215 – 220.

[34] T. A. Elmitwalli, J. Soellner, A. D. Keizer, H. Bruning, G. Zeeman, G. Lettinga, Biodegradability and change of physical characteristics of particles during anaerobic digestion of domestic sewage, Water Research 35 (5) (2001) 1311 – 1317.

[35] R. Higbie, The rate of absorption of a pure gas into still liquid during short periods of exposure, Trans. Am. Inst. Chem. Eng. 31 (2).

[36] F. J. Montes, M. A. Galan, R. L. Cerro, Mass transfer from oscillating bubbles in bioreactors, Chem. Eng. Sci. 54 (1999) 3127–3136.

[37] N. Frössling, Übber die verdünstung fallenden trop fen (Evaporation of falling drops), Gerlands Beitrage zur Geophys. von Gerl. 52 (1938) 170–216.

[38] A. Tomiyama, I. Kataoka, I. Zun, T. Sakaguchi, Drag Coefficients of Single bubbles under Normal and Micro Gravity Conditions, Japan Soc. Mech. Eng. Int. J. 41 (2) (1998) 472–479.

[39] M. K. AL-Mashhadani, S. J. Wilkinson, W. B. Zimmerman, Airlift bioreactor for biological applications with microbubble mediated transport processes, Chem. Eng. Sci. 137 (2015) 243–253.

[40] I. Díaz, C. Pérez, N. Alfaro, F. Fdz-Polanco, A feasibility study on the bioconversion of CO2 and H2 to biomethane by gas sparging through polymeric membranes, Bioresour. Technol. 185 (2015) 246–253.

[41] I. Martin-Garcia, V. Monsalvo, M. Pidou, P. Le-Clech, S. Judd, E. McAdam, B. Jefferson, Impact of membrane configuration on fouling in anaerobic membrane bioreactors, Journal of Membrane Science 382 (1–2) (2011) 41 – 49.

[42] A. Robles, M. Ruano, J. Ribes, A. Seco, J. Ferrer, Mathematical modelling of filtration in submerged anaerobic {MBRs} (SAnMBRs): Long-term validation, Journal of Membrane Science 446 (2013) 303 – 309.

[43] C. Shin, P. L. McCarty, J. Kim, J. Bae, Pilot-scale temperate-climate treatment of domestic wastewater with a staged anaerobic fluidized membrane bioreactor (SAF-MBR), Bioresource Technology 159 (2014) 95 – 103.

[44] G. Luo, I. Angelidaki, Co-digestion of manure and whey for in situ biogas upgrading by the addition of H2: Process performance and microbial insights, Appl. Microbiol. Biotechnol. 97 (3) (2013) 1373–1381.

[45] G. Luo, W. Wang, I. Angelidaki, Anaerobic Digestion for Simultaneous Sewage Sludge Treatment and CO Biomethanation: Process Performance and Microbial Ecology, Environmental Science & Technology 47 (18) (2013) 10685–10693.

[46] W. Wang, L. Xie, G. Luo, Q. Zhou, I. Angelidaki, Performance and microbial community analysis of the anaerobic reactor with coke oven gas biomethanation and in situ biogas upgrading, Bioresour. Technol. 146 (2013) 234–239.

[47] T. B, A. A. M., Z. Yue, C. J. P. J., H. S., B. C. J., Simultaneous biomethanisation of endogenous and imported CO_2 in organically loaded anaerobic digesters, Applied Energy 247 (2019) 670 – 681.

[48] S. Savvas, J. Donnelly, T. Patterson, Z. S. Chong, S. R. Esteves, Biological methanation of CO_2 in a novel biofilm plug-flow reactor: A high rate and low parasitic energy process, Applied Energy 202 (2017) 238 – 247.

[49] B. Lew, S. Tarre, M. Beliavski, C. Dosoretz, M. Green, Anaerobic membrane bioreactor (AnMBR) for domestic wastewater treatment, Desalination 243 (1) (2009) 251 – 257.

[50] J. Gouveia, F. Plaza, G. Garralon, F. Fdz-Polanco, M. Peña, Long-term operation of a pilot scale anaerobic membrane bioreactor (AnMBR) for the treatment of municipal wastewater under psychrophilic conditions, Bioresource Technology 185 (2015) 225 – 233.

[51] C. Ramos, A. García, V. Diez, Performance of an AnMBR pilot plant

treating high-strength lipid wastewater: Biological and filtration processes, Water Research 67 (2014) 203 – 215.